Published in final edited form as:
Biochem J. ; 421(1): 51–58. doi:10.1042/BJ20090242.

Mitochondrial peroxiredoxin 3 is more resilient to hyperoxidation than cytoplasmic peroxiredoxins

Andrew G. COX[*], **Andree G. Pearson**[*], **Juliet M. Pullar**[*], **Thomas J. Jönsson**[†], **W. Todd Lowther**[†], **Christine C. Winterbourn**[*], and **Mark B. Hampton**[*,1]

[*]Free Radical Research Group and National Research Centre for Growth and Development, Department of Pathology, University of Otago, Christchurch, New Zealand [†]Center for Structural Biology and Department of Biochemistry, Wake Forest University School of Medicine, Winston-Salem, NC, U.S.A.

Abstract

The Prxs (peroxiredoxins) are a family of cysteine-dependent peroxidases that decompose hydrogen peroxide. Prxs become hyperoxidized when a sulfenic acid formed during the catalytic cycle reacts with hydrogen peroxide. In the present study, Western blot methodology was developed to quantify hyperoxidation of individual 2-Cys Prxs in cells. It revealed that Prx 1 and 2 were hyperoxidized at lower doses of hydrogen peroxide than would be predicted from *in vitro* data, suggesting intracellular factors that promote hyperoxidation. In contrast, mitochondrial Prx 3 was considerably more resistant to hyperoxidation. The concentration of Prx 3 was estimated at 125 μM in the mitochondrial matrix of Jurkat T-lymphoma cells. Although the local cellular environment could influence susceptibility, purified Prx 3 was also more resistant to hyperoxidation, suggesting that despite having C-terminal motifs similar to sensitive eukaryote Prxs, other structural features must contribute to the innate resilience of Prx 3 to hyperoxidation.

Keywords

hydrogen peroxide; mitochondria; peroxiredoxin; oxidative stress; sulfenic acid; thiol

INTRODUCTION

Prxs (peroxiredoxins) are abundant antioxidant enzymes that use an active site cysteine to catalyse the reduction of peroxides [1]. Mammals have six Prxs grouped into three classes depending on the mechanism by which they breakdown peroxides. Prxs 1–4 belong to the typical 2-Cys class that contain two conserved cysteine residues: the peroxidative and the resolving. During their catalytic cycle, the peroxidative cysteine is oxidized to a sulfenic acid. It then condenses with the second resolving cysteine of an adjacent monomer to form

[1] To whom correspondence should be addressed (mark.hampton@otago.ac.nz)..

AUTHOR CONTRIBUTIONS

Andrew Cox was responsible for the majority of the experimental work and writing the first draft of the manuscript. Andree Pearson contributed to development of the method for measuring hyperoxidized peroxiredoxins and initial experimental results using this technique. Juliet Pullar performed the experiments involving continuous generation of hydrogen peroxide. Thomas Jönsson and Todd Lowther provided Figure 8 and they contributed to the discussion relating to sequence differences in peroxiredoxin 3 and susceptibility to hyperoxidation. Christine Winterbourn contributed to the design and interpretation of experimental results and editing of the manuscript. Mark Hampton had overall responsibility for the project and contributed to design and interpretation of experimental results and editing of the manuscript.

an intermolecular dimer that thioredoxin reduces to complete the catalytic cycle (Figure 1). The 2-Cys Prxs are distributed in various compartments within the cell; Prx 1 and 2 are cytoplasmic, Prx 3 resides in the mitochondria and Prx 4 is in the endoplasmic reticulum.

Whereas prokaryote Prxs are very effective at catalytic consumption of peroxides, studies of eukaryotic Prxs revealed sensitivity to inactivation in the presence of excess peroxide [2]. The sulfenic acid generated during catalysis can react with a second peroxide to generate a sulfinic acid in a process termed hyperoxidation [3-5] (Figure 1). Sequence alignment revealed that conserved GGLG and YF motifs in eukaryote Prxs promote hyperoxidation by hindering the local unfolding necessary for disulfide formation with the resolving cysteine [6]. The evolution of less robust Prxs suggests these proteins may have acquired additional functions. Wood et al. [6] advanced the floodgate model that proposes eukaryotic Prxs become hyperoxidized following a transient peroxide burst, thereby facilitating peroxide-mediated signalling. Also, the intricate oligomeric structures of these proteins seem unduly complex for a peroxide-removal system and there is a lack of redundancy as shown by knockout mouse models, particularly between the cytoplasmic Prxs 1 and 2 [7-9], indicating specific roles for each. There is evidence that hyperoxidized Prxs can function as molecular chaperones [10-13], and their abundance and reactivity makes them ideal peroxide sensors that could facilitate the oxidation of less reactive thiol proteins [14].

Although the relative sensitivities of prokaryote and eukaryote Prxs to hyperoxidation are well known, there has been no systematic study comparing the different mammalian Prxs. This is in part due to the technical challenge of comparing the redox state of several Prxs within an individual cell or tissue. The most commonly used technique to detect hyperoxidized Prx relies on 2D (two dimensional) electrophoresis and MS to identify spots with a more acidic isoelectric point [3-5,15,16]. Hyperoxidized Prxs can also be detected using an antibody raised to a sulphonylated peptide derived from the conserved active site sequence present in 2-Cys Prx proteins [17]. However, such an antibody does not easily distinguish between individual Prx members, making comparative analyses difficult. Furthermore, the antibody does not give any indication of the proportion of Prx that is hyperoxidized. In this study, we have taken advantage of the observation that reduced Prxs immediately oxidize following cell lysis [18]. Oxidation results in formation of an intermolecular disulfide bond visualized as a dimer Prx on a non-reducing gel. Western blotting allows assessment of individual Prxs. Hyperoxidized Prxs are unable to dimerize and remain in the monomeric form following cell lysis. Using this technique, we observed dramatic differences in sensitivity to hyperoxidation between the cytosolic Prxs and mitochondrial Prx 3, both in cells and with purified protein, suggesting sequence variation contributes to the resilience of Prx 3.

EXPERIMENTAL

Materials

The Jurkat T lymphoma and HeLa cervical adenocarcinoma cell lines were obtained from American Type Culture Collection. Peroxidase-conjugated anti-rabbit antibody, DTT (dithiothreitol), NEM (*N*-ethylmaleimide), catalase and glucose oxidase were purchased from Sigma (St Louis, MO, U.S.A.). Recombinant Prx 1 and Prx 3 protein as well as primary antibodies to Prx 1, Prx 2, Prx 3 and Prx-SO_2H were purchased from Young and Abfrontier (Seoul, Korea). Micro Bio-Spin® 6 chromotography columns were purchased from Bio-Rad. Complete™ protease inhibitors were from Roche Diagnostics. All other chemicals and reagents were from Sigma and BDH Laboratory Supplies (Poole, U.K.). All water was deionized and ultrafiltered using a Milli-Q filtration system.

Cell culture

Jurkat cells were cultured in RPMI-1640 containing 10% fetal bovine serum, 100 units/ml penicillin and 100 μg/ml streptomycin. Jurkat cells were seeded at 1×10^6 cells/ml in fresh media and incubated for 1 h prior to treatment. HeLa cells were grown in DMEM (Dulbecco's minimum essential medium) containing 10% fetal bovine serum, 100 units/ml penicillin and 100 μg/ml streptomycin. HeLa cells were treated at 80% confluence in fresh DMEM containing 10% fetal bovine serum. Cells were maintained at 37°C in a humidified atmosphere with 5% CO_2. All incubations of cells with hydrogen peroxide were performed at 37°C.

Western blot analysis of Prxs

Treated Jurkat cells (1×10^6) were washed in ice-cold PBS and resuspended in extract buffer (40 mM Hepes, 50 mM NaCl, 1 mM EDTA, 1 mM EGTA and protease inhibitors, pH 7.4) containing 1% CHAPS, in order to monitor Prx hyperoxidation, or extract buffer containing 100 mM NEM, in order to monitor Prx dimerization. Samples containing NEM were incubated for 10 min before 1% CHAPS was added to lyse the cells. After 10 min incubation with CHAPS, the insoluble material was removed from cellular extracts by centrifugation at 16000 ***g*** for 5 min. Extracts were added to sample buffer (final concentration: 2% SDS, 10% glycerol and 62.5 mM Tris, pH 6.8) and run on SDS/PAGE in non-reducing conditions, or with 50 mM DTT when reducing conditions were required. Transfer of proteins to PVDF and detection of proteins using chemiluminescence were performed using standard techniques. Chemiluminescence images were captured using a Chemi-Doc XRS scanner (Bio-Rad). Relative band densities of Western blots were determined using Quantity One (Bio-Rad).

Quantifying mitochondrial volume in Jurkat T lymphocytes

Mitochondrial volume in Jurkat cells was measured using the potentiometric dye TMRE (tetramethylrhodamine ethyl ester). Jurkat cells were stained with 50 nM TMRE for 15 min before being imaged by confocal microscopy using a Leica TCS SP5 confocal microscope (Leica Microsystems). Z-stack images of individual Jurkat cells were analysed to calculate the mitochondrial volume (% TMRE fluorescence in cell). The mitochondrial volume of Jurkat cells was determined by calculating the percentage of red pixels within the cross-section of an individual cell (Adobe Photoshop™) over the entire z-stack.

Monitoring acidic shifts of Prxs by 2D gel electrophoresis

Treated Jurkat cells were harvested, washed in PBS and then lysed in extract buffer containing 1% CHAPS. The soluble extract was passed through a spin column pre-equilibrated with rehydration buffer [7 M urea, 2 M thiourea, 10 mM DTT, 4% (w/v) CHAPS, 0.2% (v/v) Biolytes 3–10 and Bromophenol Blue] and loaded onto immobilized pH gradient strips pH 3–10 (Bio-Rad). Isoelectric focusing was carried out on a Bio-Rad Protean IEF cell according to the manufacturer's instructions. Focused strips were reduced in equilibration buffer [6 M urea, 36% (v/v) glycerol, 2% (w/v) SDS, 50 mM Tris/HCl, pH 6.8] containing 25 mM DTT for 10 min, followed by alkylation in equilibration buffer containing 50 mM iodoacetamide for 10 min, before being separated by SDS/15% PAGE and Western blotted as outlined above.

Continuous generation of hydrogen peroxide

An enzymatic system generating steady state levels of exogenous hydrogen peroxide was used as described in [19]. In brief, hydrogen peroxide was generated by the enzymatic oxidation of glucose by glucose oxidase in the presence of catalase, which was included to control hydrogen peroxide levels. For all experiments, glucose (5 mM) and glucose oxidase

were added to PBS (pH 7.4) at 37°C with constant mixing. Catalase was added and the solution was allowed to equilibrate before the addition of cells. The concentration of hydrogen peroxide was measured throughout the experiment using a hydrogen peroxide electrode (World Precision Instruments).

UV-B exposure of cells

Jurkat cells in Hanks buffered saline solution were exposed to the UV transilluminator of a Chemi-Doc XRS equipped with 6 × 302 nm lamps (Bio-Rad) for the indicated periods of time before cells were harvested in the presence or absence of NEM as described above.

In vitro Prx studies

Prx 2 was purified from human erythrocytes as previously described [18] based on the method of Lim et al. [20]. Recombinant human Prx 1 and Prx 3 (minus the mitochondrial leader sequence) were obtained from Young and Abfrontier. Purified Prx 1, 2 and 3 were reduced with 25 mM DTT for 30 min at room temperature (20°C). Excess DTT was removed by passing the Prxs through spin columns pre-equilibrated with PBS containing 10 μg/ml bovine catalase, which is necessary to prevent the reoxidation of the reduced Prxs as they pass through the column matrix in the absence of reductant [18]. The reduced Prxs (7 μM) were treated with various concentrations of hydrogen peroxide at 20°C for 10 min. Reactions were stopped with 25 mM NEM and samples were added to sample buffer and run on SDS/15% PAGE. Proteins were detected by Coomassie Blue or silver stain. Western blotting of the purified protein was performed using standard techniques.

Statistics

Values are shown as the mean and standard error of three or more independent experiments, and all blots are representative of at least three independent experiments. Statistical analyses were performed with the software package SigmaStat (Systat).

RESULTS

Prx expression and localization in Jurkat cells

The concentration of each Prx isoform was estimated by immunoblotting and comparing the band intensity of whole cell lysates with amounts of purified Prx. Quantification of band intensities revealed that Prx 1 was the most abundant isoform in Jurkat whole cell lysates, with a concentration of approx. 5 μg/mg soluble protein, whereas Prx 2 was present at approximately 2 μg/mg (Figure 2A). We calculate the volume of a Jurkat cell to be approx. 0.5 pl (sphere with diameter of 10 μm) and 1×10^7 cells contain 1 mg of protein. From these parameters it can be estimated that 1×10^7 Jurkat cells contain 330 pmoles of Prx 1 and 2 combined (molecular mass 21 kDa) at a concentration of 65 μM. This is an average value that ignores compartmentalization, and local cytoplasmic concentrations could be higher. Prx 3 was present at approx. 2 μg/mg of soluble protein (Figure 2A). Using confocal microscopy and the potentiometric dye TMRE, which selectively accumulates in the mitochondria, we estimated that mitochondria constitute 15% of the volume of Jurkat cells (Figure 2B). Therefore, the 95 pmoles of Prx 3 in 1×10^7 Jurkat cells will be at a concentration of approx. 125 μM.

Spontaneous dimerization during cell harvest provides a method to monitor hyperoxidation of specific Prxs

When Jurkat cells were exposed to increasing doses of hydrogen peroxide (0–400 μM) for 10 min, we observed a dose-dependent increase in Prx hyperoxidation as visualized with an antibody raised against the hyperoxidized cysteine-containing sequence (Figure 3A).

Unfortunately, the antibody does not distinguish between different Prxs, and it is not possible to determine the percentage of the Prxs that are hyperoxidized. We wanted to establish a method to monitor individual Prx family members and detect the degree of hyperoxidation. Under reducing conditions, the Prxs separate as monomers. The presence of a reductant is critical, because Prxs are extremely sensitive to adventitious hydrogen peroxide in lysis buffers or desalting columns and are immediately oxidized following cell lysis [18]. The high reactivity of Prxs with hydrogen peroxide ($k = 10^7\ M^{-1} \cdot s^{-1}$) facilitates dimerization upon cell lysis [18], whereas hyperoxidation does not occur during cell lysis, as the process is slow and requires catalytic cycling [5]. This is reflected in the transition of the monomer to the intermolecular disulfide-bonded dimer (~42 kDa) on a non-reducing gel (Figure 3B). However, if the peroxidative cysteine is hyperoxidized, then the Prx will be unable to dimerize following cell lysis. This is illustrated in Figure 3B, where addition of 20 μM hydrogen peroxide caused some of Prx 1 to be trapped as a monomer.

Cytosolic Prxs are more susceptible to hyperoxidation than mitochondrial Prx 3 in cells exposed to hydrogen peroxide

To compare the relative susceptibility of Prxs 1–3 to hyperoxidation, Jurkat cells were treated for 10 min with a range of hydrogen peroxide concentrations before protein extraction and separation on a non-reducing gel. For all three Prxs, treatment of cells with increasing concentrations of hydrogen peroxide caused an increase in the presence of the hyperoxidized monomer (Figure 4A). However, there was a dramatic difference in relative sensitivities, with mitochondrial Prx 3 considerably more resistant than Prx 1 and 2 (Figures 4A and 4B).

This method was validated by 2D electrophoresis and Western blotting, taking advantage of the acidic shift exhibited by hyperoxidized Prxs. The studies confirmed that Prxs 1 and 2 were completely converted into an acidic form following exposure to 200 μM hydrogen peroxide, whereas only 25% of Prx 3 shifted to the acidic state (Figure 5). Western blotting of the 2D gels with the Prx-SO_2H antibody verified that the acidic spots were indeed hyperoxidized forms of the Prxs (Figure 5).

To confirm that the differences in susceptibility were not specific to Jurkat T lymphoma cells we examined the response of HeLa cervical adenocarcinoma cells to hydrogen peroxide. There was a dose-dependent increase in hyperoxidized monomer using the Prx-SO_2H antibody (Supplementary Figure S1 at http://www.BiochemJ.org/bj/421/bj4210051add.htm). The cytosolic Prxs displayed similar sensitivities, with the majority of each isoform being hyperoxidized with 120 μM hydrogen peroxide (Supplementary Figure S1). As in Jurkat cells, mitochondrial Prx 3 was very resistant to hyperoxidation, with only a small fraction detectable following treatment with 160 μM hydrogen peroxide (Supplementary Figure S1).

Glucose oxidase was used to compare the effects of steady-state generation of hydrogen peroxide with the bolus additions described above. A steady-state of 10–15 μM hydrogen peroxide was established in the presence of catalase [19]. Cells were then removed at 0, 10, 20 and 40 min and analysed by Western blotting in non-reducing conditions. Hyperoxidation of Prx 2 was evident within 20 min and the majority of Prx 1 was hyperoxidized after 40 min (Figure 6A). In contrast, Prx 3 showed no signs of hyperoxidation (Figure 6A).

UV-B radiation was also used as it has been shown to generate hydrogen peroxide intracellularly in all compartments including the mitochondria [22-26]. Jurkat cells were exposed to UV-B radiation for 0, 5, 10 and 15 min before being harvested. Western blot analysis in non-reducing conditions demonstrated that the cytosolic Prxs became

hyperoxidized, with Prx 2 again more sensitive than Prx 1, and mitochondrial Prx 3 remained resistant to hyperoxidation (Figure 6B).

Differential sensitivities of purified Prxs to hyperoxidation

To determine whether there are intrinsic differences in the propensity of Prxs to hyperoxidation, purified Prxs (7 μM) were exposed to a range of hydrogen peroxide concentrations for 10 min before further reaction was prevented with 25 mM NEM, and samples were run on SDS/PAGE. Gels were subsequently silver stained or probed for Prx hyperoxidation by immunoblot against Prx-SO_2H. Prx 1 formed dimers and higher molecular mass complexes at low concentrations of hydrogen peroxide (Figure 7A). This is consistent with previous studies demonstrating that this protein contains an additional cysteine which can enable higher order disulfide aggregates *in vitro* [13]. Immunoblot analysis revealed that the sulfinic acid species were present in the higher molecular mass complexes of Prx 1 (Figure 7B). The Prx 2 dimer was the major product at the lowest dose of hydrogen peroxide, with the dimer containing a considerable number of hyperoxidized groups, presumably representing a single disulfide bond with a sulfinic acid on the other peroxidatic cysteine. The hyperoxidized monomer was more prominent at higher doses (Figure 7). Interestingly, Prx 3 formed dimer at all hydrogen peroxide concentrations but showed little immunoreactivity with the Prx-SO_2H antibody, except at the highest dose, and only in the dimer (Figure 7).

DISCUSSION

In this study a redox immunoblotting technique was developed to measure the hyperoxidation of individual Prxs. It revealed that Prx 3 is considerably more resistant to hyperoxidation than Prx 1 and Prx 2, which are both cytoplasmic members of the typical 2-Cys peroxiredoxin family. Prx 3 functions within the mitochondrial matrix and a wealth of evidence indicates that mitochondria have unique redox characteristics that operate independently of the cytosol [27]. We have previously shown selective Prx 3 oxidation during the initiation of receptor-mediated apoptosis [28] and upon exposure to thioredoxin reductase inhibitors [29] and pro-apoptotic isothiocyanates [30]. However, although compartmentalization within mitochondria could contribute to this difference, *in vitro* studies with purified Prx 3 indicated an innate resilience more commonly seen with prokaryotic Prxs.

Wood et al. [6] showed that eukaryotic Prxs are more sensitive to hyperoxidation and that their C-terminal extension promotes hyperoxidation by impairing local unfolding, thereby increasing the lifetime of the active site sulfenic acid for reaction with a second molecule of hydrogen peroxide. Truncations of the C-terminus are known to protect Prxs from hyperoxidation [6,31,32]. Modifications that lead to a more flexible C-terminal loop in Prx 3 would be expected to increase the rate of disulfide bond formation between the peroxidative and resolving cysteines, thereby decreasing the opportunity for hyperoxidation. Examination of the primary sequence of Prxs 1–3 indicates extensive homology between the proteins, including identical active sites. However, there are significant side chain substitutions at the C-termini, in particular the amino acids three, five, seven and nine residues downstream of the resolving cysteine (Figure 8), which are also conserved in the Prx 3 sequences of mice and zebrafish (not shown). Based on the substitution of asparagine and aspartate for two glycine residues and a proline residue for aspartate, one might anticipate the C-terminus of Prx 3 to lose flexibility and become more sensitive to hyperoxidation, however, this is the opposite of what we observed. N-terminal acetylation has been reported to influence Prx hyperoxidation [33], suggesting other regions of the protein could also contribute. While it may prove complex, a more in-depth investigation of structural properties on Prx sensitivity to hyperoxidation is warranted.

An alternate possibility is that the mitochondrial environment could protect Prx 3 from hyperoxidation by restricting exposure to hydrogen peroxide, or limiting catalytic turnover. The first scenario seems unlikely because of the high levels of hydrogen peroxide used in this study. The mitochondrial hydrogen peroxide concentration in cells exposed to external hydrogen peroxide is estimated to be one-third that of cytoplasmic levels [33a], yet the results from the present study indicated greater than 20-fold increased resistance of Prx 3. In the second scenario, limited turnover by the mitochondrial thioredoxin system would decrease the opportunity for hyperoxidation, similar to the manner by which low thioredoxin reductase activity protects Prx 2 hyperoxidation in the erythrocyte [34]. This would be visualized as an increase in disulfide-linked Prx 3, which we have previously measured with some apoptotic stimuli and thioredoxin reductase inhibitors [28-30], but there was no increase in Prx 3 dimer formation following hydrogen peroxide treatment (results not shown).

The cytoplasmic Prxs were completely hyperoxidized in cells at relatively low doses of hydrogen peroxide. Kinetic studies with purified Prx 1, thioredoxin and a steady-state of 1 μM hydrogen peroxide indicated that hyperoxidation occurs 1 in every 1300 turnovers of Prx [5]. We observed almost complete Prx hyperoxidation with 20 μM hydrogen peroxide. This corresponds with 20 nmoles in 1×10^6 cells that contain 33 pmoles of Prx 1 and 2, so if the hydrogen peroxide only reacted with these two Prxs there would be 1 hyperoxidation event per 600 turnovers. *In vivo*, however, there will be other competing reactions; therefore, hyperoxidation was more efficient than would be predicted from the *in vitro* data. Further research is required to determine if factors such as oligomeric state, post-translational modifications and protein–protein interactions facilitate hyperoxidation in a cellular environment.

Our method for quantifying hyperoxidation of individual Prxs will be generally applicable to cell and tissue samples. The method relies on the propensity of reduced Prxs to form intermolecular disulfides following cell lysis, so will be applicable to all 2-Cys Prxs that have specific antibodies. One potential limitation would be the formation of a Prx complex that had one hyperoxidized peroxidatic cysteine and one reduced or disulfide-linked peroxidatic cysteine, which would run as a dimer on the non-reducing gel (or more complex oligomeric structures such as those observed for purified Prx 1). In this study these species were only detected with pure protein. The presence of reductants *in vivo* will enable continued Prx cycling and facilitate complete hyperoxidation. In what may be a restricted example, we observed the hyperoxidized Prx 2 dimer as a minor component in erythrocytes exposed to high concentrations of hydrogen peroxide, with the catalytic activity of erythrocyte Prx 2 restricted by low levels of active thioredoxin reductase [34]. A recent study also identified low levels of hyperoxidized dimer in hearts perfused with hydrogen peroxide [35].

The usual method for measuring Prx hyperoxidation using an antibody raised against a sulfonylated Prx peptide does not easily distinguish individual Prxs. Subtle differences in molecular mass may make it possible to separate Prxs by SDS/PAGE [17], but this still does not provide information on the extent of hyperoxidation. Acidic shifts of hyperoxidized Prxs can be detected by 2D electrophoresis, but this technique is cumbersome for multiple samples and there is the potential for interference from other post-translational modifications such as phosphorylation. Nevertheless, our conclusion that Prx 3 is more resistant to hyperoxidation than the cytosolic Prxs supports previous studies that used the 2D electrophoresis approach [3,15,36]. For example, Rabilloud and co-workers showed that hyperoxidized Prx 3 is poorly retroreduced in Jurkat cells, whereas Prx 2 is repaired rapidly [3,4]. Rabilloud et al. [3] also found that Prx 2 was more sensitive to hyperoxidation than Prx 3 in Jurkat cells exposed to moderate levels of hydrogen peroxide generated by glucose

oxidase. Of note, a significant amount of acidic Prx 3 was observed in resting Jurkat cells. This was not detectable with our method, highlighting potential complications of ascribing acidic mobility shifts to hyperoxidation.

The observations in this study do not exclude the possibility that hyperoxidized Prx 3 will be detectable *in vivo*. Indeed, hyperoxidized Prx 3 is observed in cultured cells following prolonged exposure to high levels of hydrogen peroxide or drugs that generate hydrogen peroxide [3,4,17,37], and in the liver of aged rats [46]. Although the rate of formation may be considerably slower in comparison with cytoplasmic Prxs, the rate of clearance will be a key factor. Hyperoxidized Prxs are repaired (retroreduced) very slowly by the ATP-dependent sulfinyl reductase sulfiredoxin [38,39]. Despite the slow rate (k_{cat} = 0.2−0.5 min^{-1}) [39,40], sulfiredoxin is essential in re-establishing the antioxidant function of Prxs following acute oxidative stress [41-43].

The resistance that Prx 3 exhibits to hyperoxidation is likely to have biological ramifications. It is well known that hyperoxidized Prx 3 remains inactive for an extended period before it is retro-reduced [3,4,15,17,44,45]. Sulfiredoxin is present in the cytosol [39], however, it slowly trafficks to the mitochondria following oxidative stress [45]. If Prx 3 was readily hyperoxidized, this would inactivate a key mitochondrial antioxidant enzyme for a prolonged period. This is particularly problematic for Prx 3, especially because it resides in an environment of elevated endogenous generation of hydrogen peroxide [47]. Also, the floodgate hypothesis proposed by Wood et al. [6] suggests that hyperoxidation of Prxs during peroxide bursts may allow H_2O_2 to act as a second messenger during signal transduction. As such, the sensitivity of some Prxs to hyperoxidation is seen as a ‘gain of function’ that enables Prxs to have dual functionality as both peroxide scavengers and regulators of peroxide-mediated signal transduction. The fact that Prx 3 is more resilient to hyperoxidation suggests alternate mechanisms or alternate roles compared with other members of the Prx family.

Supplementary Material

Refer to Web version on PubMed Central for supplementary material.

Acknowledgments

We thank Dr David Collings (Department of Biological Sciences, University of Canterbury) for performing confocal microscopy.

FUNDING

This project was supported by the Health Research Council of New Zealand, the National Research Centre for Growth and Development and by National Institutes of Health [grant number R01GM072866] (to W. T. L.). A. G. C. is a recipient of a Top Achiever doctoral scholarship from the Tertiary Education Commission of New Zealand.

Abbreviations used

2D	two dimensional
DMEM	Dulbecco’s minimum essential medium
DTT	dithiothreitol
NEM	*N*-ethylmaleimide
Prx	peroxiredoxin
TMRE	tetramethylrhodamine ethyl ester

REFERENCES

1. Wood ZA, Schroder E, Harris JR, Poole LB. Structure, mechanism and regulation of peroxiredoxins. Trends Biochem. Sci. 2003; 28:32–40. [PubMed: 12517450]
2. Chae HZ, Chung SJ, Rhee SG. Thioredoxin-dependent peroxide reductase from yeast. J. Biol. Chem. 1994; 269:27670–27678. [PubMed: 7961686]
3. Rabilloud T, Heller M, Gasnier F, Luche S, Rey C, Aebersold R, Benahmed M, Louisot P, Lunardi J. Proteomics analysis of cellular response to oxidative stress – evidence for *in vivo* overoxidation of peroxiredoxins at their active site. J. Biol. Chem. 2002; 277:19396–19401. [PubMed: 11904290]
4. Chevallet M, Wagner E, Luche S, van Dorsselaer A, Leize-Wagner E, Rabilloud T. Regeneration of peroxiredoxins during recovery after oxidative stress – only some overoxidized peroxiredoxins can be reduced during recovery after oxidative stress. J. Biol. Chem. 2003; 278:37146–37153. [PubMed: 12853451]
5. Yang KS, Kang SW, Woo HA, Hwang SC, Chae HZ, Kim K, Rhee SG. Inactivation of human peroxiredoxin I during catalysis as the result of the oxidation of the catalytic site cysteine to cysteine-sulfinic acid. J. Biol. Chem. 2002; 277:38029–38036. [PubMed: 12161445]
6. Wood ZA, Poole LB, Karplus PA. Peroxiredoxin evolution and the regulation of hydrogen peroxide signaling. Science. 2003; 300:650–653. [PubMed: 12714747]
7. Neumann CA, Krause DS, Carman CV, Das S, Dubey DP, Abraham JL, Bronson RT, Fujiwara Y, Orkin SH, Van Etten RA. Essential role for the peroxiredoxin Prdx1 in erythrocyte antioxidant defence and tumour suppression. Nature. 2003; 424:561–565. [PubMed: 12891360]
8. Lee TH, Kim SU, Yu SL, Kim SH, Park DS, Moon HB, Dho SH, Kwon KS, Kwon HJ, Han YH, et al. Peroxiredoxin II is essential for sustaining life span of erythrocytes in mice. Blood. 2003; 101:5033–5038. [PubMed: 12586629]
9. Li L, Shoji W, Takano H, Nishimura N, Aoki Y, Takahashi R, Goto S, Kaifu T, Takai T, Obinata M. Increased susceptibility of MER5 (peroxiredoxin III) knockout mice to LPS-induced oxidative stress. Biochem. Biophys. Res. Commun. 2007; 355:715–721. [PubMed: 17316558]
10. Jang HH, Lee KO, Chi YH, Jung BG, Park SK, Park JH, Lee JR, Lee SS, Moon JC, Yun JW, et al. Two enzymes in one; two yeast peroxiredoxins display oxidative stress-dependent switching from a peroxidase to a molecular chaperone function. Cell. 2004; 117:625–635. [PubMed: 15163410]
11. Moon JC, Hah YS, Kim WY, Jung BG, Jang HH, Lee JR, Kim SY, Lee YM, Jeon MG, Kim CW, et al. Oxidative stress-dependent structural and functional switching of a human 2-Cys peroxiredoxin isotype II that enhances HeLa cell resistance to H_2O_2-induced cell death. J. Biol. Chem. 2005; 280:28775–28784. [PubMed: 15941719]
12. Chuang MH, Wu MS, Lo WL, Lin JT, Wong CH, Chiou SH. The antioxidant protein alkylhydroperoxide reductase of *Helicobacter pylori* switches from a peroxide reductase to a molecular chaperone function. Proc. Natl. Acad. Sci. U.S.A. 2006; 103:2552–2557. [PubMed: 16481626]
13. Lee W, Choi KS, Riddell J, Ip C, Ghosh D, Park JH, Park YM. Human peroxiredoxin 1 and 2 are not duplicate proteins: the unique presence of CYS83 in Prx1 underscores the structural and functional differences between Prx1 and Prx2. J. Biol. Chem. 2007; 282:22011–22022. [PubMed: 17519234]
14. Winterbourn CC, Hampton MB. Thiol chemistry and specificity in redox signaling. Free Radic. Biol. Med. 2008; 45:549–561. [PubMed: 18544350]
15. Mitsumoto A, Takanezawa Y, Okawa K, Iwamatsu A, Nakagawa Y. Variants of peroxiredoxins expression in response to hydroperoxide stress. Free Radical Biol. Med. 2001; 30:625–635. [PubMed: 11295360]
16. Mitsumoto A, Nakagawa Y, Takeuchi A, Okawa K, Iwamatsu A, Takanezawa Y. Oxidized forms of peroxiredoxins and DJ-1 on two-dimensional gels increased in response to sublethal levels of paraquat. Free Radical Res. 2001; 35:301–310. [PubMed: 11697128]
17. Woo HA, Kang SW, Kim HK, Yang KS, Chae HZ, Rhee SG. Reversible oxidation of the active site cysteine of peroxiredoxins to cysteine sulfinic acid – immunoblot detection with antibodies specific for the hyperoxidized cysteine-containing sequence. J. Biol. Chem. 2003; 278:47361–47364. [PubMed: 14559909]

18. Peskin AV, Low FM, Paton LN, Maghzal GJ, Hampton MB, Winterbourn CC. The high reactivity of peroxiredoxin 2 with H_2O_2 is not reflected in its reaction with other oxidants and thiol reagents. J. Biol. Chem. 2007; 282:11885–11892. [PubMed: 17329258]
19. Pantopoulos K, Mueller S, Atzberger A, Ansorge W, Stremmel W, Hentze MW. Differences in the regulation of iron regulatory protein-1 (IRP-1) by extra- and intracellular oxidative stress. J. Biol. Chem. 1997; 272:9802–9808. [PubMed: 9092514]
20. Lim YS, Cha MK, Yun CH, Kim HK, Kim K, Kim IH. Purification and characterization of thiol-specific antioxidant protein from human red blood cell:a new type of antioxidant protein. Biochem. Biophys. Res. Commun. 1994; 199:199–206. [PubMed: 8123012]
21. Wu H, Wheeler A, Zare RN. Chemical cytometry on a picoliter-scale integrated microfluidic chip. Proc. Natl. Acad. Sci. U.S.A. 2004; 101:12809–12813. [PubMed: 15328405]
22. Masaki H, Sakurai H. Increased generation of hydrogen peroxide possibly from mitochondrial respiratory chain after UVB irradiation of murine fibroblasts. J. Dermatol. Sci. 1997; 14:207–216. [PubMed: 9138478]
23. Hockberger PE, Skimina TA, Centonze VE, Lavin C, Chu S, Dadras S, Reddy JK, White JG. Activation of flavin-containing oxidases underlies light-induced production of H_2O_2 in mammalian cells. Proc. Natl. Acad. Sci. U.S.A. 1999; 96:6255–6260. [PubMed: 10339574]
24. Gniadecki R, Thorn T, Vicanova J, Petersen A, Wulf HC. Role of mitochondria in ultraviolet-induced oxidative stress. J. Cell. Biochem. 2000; 80:216–222. [PubMed: 11074592]
25. Heck DE, Vetrano AM, Mariano TM, Laskin JD. UVB light stimulates production of reactive oxygen species: unexpected role for catalase. J. Biol. Chem. 2003; 278:22432–22436. [PubMed: 12730222]
26. Gonzalez Maglio DH, Paz ML, Ferrari A, Weill FS, Czerniczyniec A, Leoni J, Bustamante J. Skin damage and mitochondrial dysfunction after acute ultraviolet B irradiation: relationship with nitric oxide production. Photodermatol. Photoimmunol. Photomed. 2005; 21:311–317. [PubMed: 16313242]
27. Go YM, Jones DP. Redox compartmentalization in eukaryotic cells. Biochim. Biophys. Acta. 2008; 1780:1273–1290. [PubMed: 18267127]
28. Cox AG, Pullar JM, Hughes G, Ledgerwood EC, Hampton MB. Oxidation of mitochondrial peroxiredoxin 3 during the initiation of receptor-mediated apoptosis. Free Radical Biol. Med. 2008; 44:1001–1009. [PubMed: 18164270]
29. Cox AG, Brown KK, Arner ES, Hampton MB. The thioredoxin reductase inhibitor auranofin triggers apoptosis through a Bax/Bak-dependent process that involves peroxiredoxin 3 oxidation. Biochem. Pharm. 2008; 76:1097–1109. [PubMed: 18789312]
30. Brown KK, Eriksson SE, Arner ES, Hampton MB. Mitochondrial peroxiredoxin 3 is rapidly oxidized in cells treated with isothiocyanates. Free Radical Biol. Med. 2008; 45:494–502. [PubMed: 18501718]
31. Koo KH, Lee S, Jeong SY, Kim ET, Kim HJ, Kim K, Song K, Chae HZ. Regulation of thioredoxin peroxidase activity by C-terminal truncation. Arch. Biochem. Biophys. 2002; 397:312–318. [PubMed: 11795888]
32. Jara M, Vivancos AP, Hidalgo E. C-terminal truncation of the peroxiredoxin Tpx1 decreases its sensitivity for hydrogen peroxide without compromising its role in signal transduction. Genes Cells. 2008; 13:171–179. [PubMed: 18233959]
33. Seo JH, Lim JC, Lee DY, Kim KS, Piszczek G, Nam HW, Kim YS, Ahn T, Yun CH, Kim K, et al. A novel protective mechanism against irreversible hyperoxidation of peroxiredoxin: N α-terminal acetylation of human peroxiredoxin II. J. Biol, Chem. 2009 doi: 10.1074/jbc.M900641200.

33a. Antunes F, Cadenas E. Estimation of H_2O_2 gradients across biomembranes. FEBS Lett. 2000; 475:121–126. [PubMed: 10858501]

34. Low FM, Hampton MB, Peskin AV, Winterbourn CC. Peroxiredoxin 2 functions as a noncatalytic scavenger of low-level hydrogen peroxide in the erythrocyte. Blood. 2007; 109:2611–2617. [PubMed: 17105810]
35. Schroder E, Brennan JP, Eaton P. Cardiac peroxiredoxins undergo complex modifications during cardiac oxidant stress. Am. J. Physiol. Heart. Circ. Physiol. 2008; 295:H425–H433. [PubMed: 18502910]

36. Phalen TJ, Weirather K, Deming PB, Anathy V, Howe AK, van der Vliet A, Jonsson TJ, Poole LB, Heintz NH. Oxidation state governs structural transitions in peroxiredoxin II that correlate with cell cycle arrest and recovery. J. Cell Biol. 2006; 175:779–789. [PubMed: 17145963]
37. Saito Y, Nishio K, Ogawa Y, Kinumi T, Yoshida Y, Masuo Y, Niki E. Molecular mechanisms of 6-hydroxydopamine-induced cytotoxicity in PC12 cells: involvement of hydrogen peroxide-dependent and -independent action. Free Radical Biol. Med. 2007; 42:675–685. [PubMed: 17291991]
38. Biteau B, Labarre J, Toledano MB. ATP-dependent reduction of cysteine-sulphinic acid by *S. cerevisiae* sulphiredoxin. Nature. 2003; 425:980–984. [PubMed: 14586471]
39. Chang TS, Jeong W, Woo HA, Lee SM, Park S, Rhee SG. Characterization of mammalian sulfiredoxin and its reactivation of hyperoxidized peroxiredoxin through reduction of cysteine sulfinic acid in the active site to cysteine. J. Biol. Chem. 2004; 279:50994–51001. [PubMed: 15448164]
40. Lee DY, Park SJ, Jeong W, Sung HJ, Oho T, Wu X, Rhee SG, Gruschus JM. Mutagenesis and modeling of the peroxiredoxin (Prx) complex with the NMR structure of ATP-bound human sulfiredoxin implicate aspartate 187 of Prx I as the catalytic residue in ATP hydrolysis. Biochemistry. 2006; 45:15301–15309. [PubMed: 17176052]
41. Bozonet SM, Findlay VJ, Day AM, Cameron J, Veal EA, Morgan BA. Oxidation of a eukaryotic 2-Cys peroxiredoxin is a molecular switch controlling the transcriptional response to increasing levels of hydrogen peroxide. J. Biol. Chem. 2005; 280:23319–23327. [PubMed: 15824112]
42. Vivancos AP, Castillo EA, Biteau B, Nicot C, Ayte J, Toledano MB, Hidalgo E. A cysteine-sulfinic acid in peroxiredoxin regulates H_2O_2-sensing by the antioxidant Pap1 pathway. Proc. Natl. Acad. Sci. U.S.A. 2005; 102:8875–8880. [PubMed: 15956211]
43. Jonsson TJ, Lowther WT. The peroxiredoxin repair proteins. Subcell. Biochem. 2007; 44:115–141. [PubMed: 18084892]
44. Lehtonen ST, Markkanen PM, Peltoniemi M, Kang SW, Kinnula VL. Variable overoxidation of peroxiredoxins in human lung cells in severe oxidative stress. Am. J. Physiol. Lung Cell. Mol. Physiol. 2005; 288:L997–L1001. [PubMed: 15626747]
45. Noh YH, Baek JY, Jeong W, Rhee SG, Chang TS. Sulfiredoxin translocation into mitochondria plays a crucial role in reducing hyperoxidized peroxiredoxin III. J. Biol. Chem. 2009; 284:8470–8477. [PubMed: 19176523]
46. Musicco C, Capelli V, Pesce V, Timperio AM, Calvani M, Mosconi L, Zolla L, Cantatore P, Gadaleta MN. Accumulation of overoxidized peroxiredoxin III in aged rat liver mitochondria. Biochim. Biophys, Acta. 2009 doi: 10.1016/j.bbabio.2009.03.002.
47. Murphy MP. How mitochondria produce reactive oxygen species. Biochem. J. 2009; 417:1–13. [PubMed: 19061483]
48. Schroder E, Littlechild JA, Lebedev AA, Errington N, Vagin AA, Isupov MN. Crystal structure of decameric 2-Cys peroxiredoxin from human erythrocytes at 1.7 Å resolution. Structure. 2000; 8:605–615. [PubMed: 10873855]

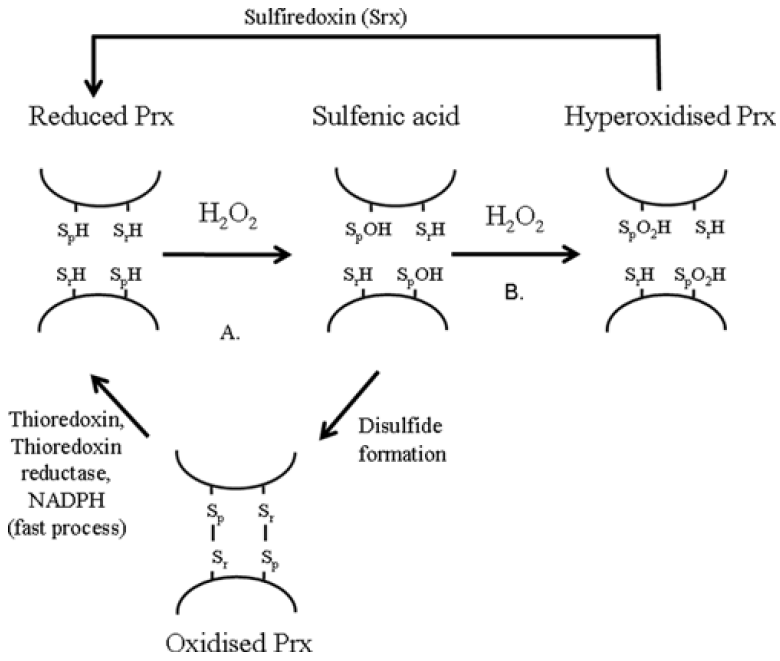

Figure 1. Hyperoxidation during the catalytic cycle of the Prxs

(**A**) The peroxidatic cysteine (S_pH) reacts with H_2O_2 to form a sulfenic acid intermediate, which can condense with the resolving cysteine on another Prx to form an intermolecular disulfide. The oxidized Prx dimer is reduced by thioredoxin to complete the catalytic cycle. (**B**) H_2O_2 can also react with the sulfenic acid intermediate to form the hyperoxidized sulfinic acid.

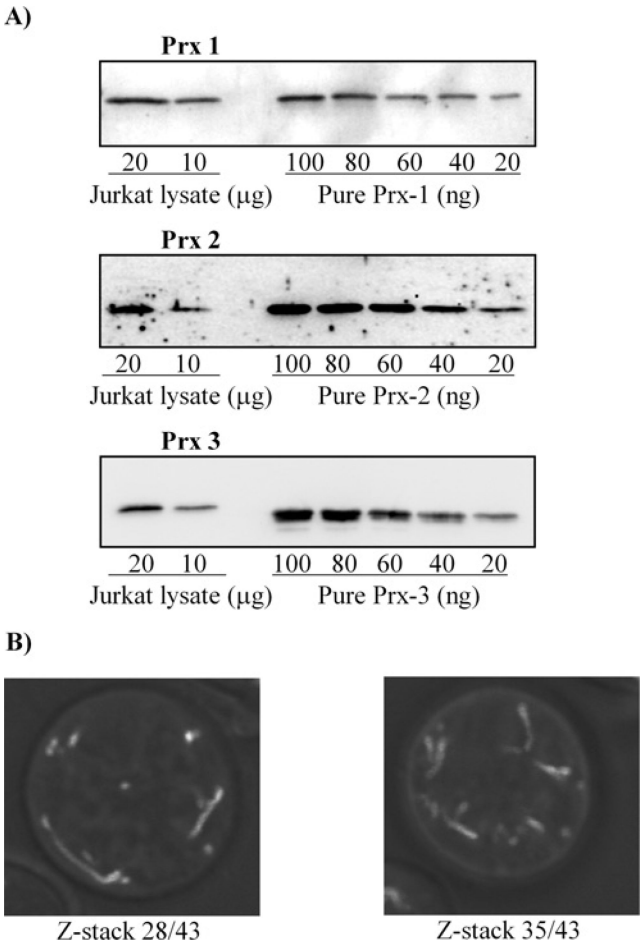

Figure 2. Expression of Prx 1, Prx 2 and Prx 3 in Jurkat cells

(**A**) Quantification of Prx 1, Prx 2 and Prx 3 concentration in Jurkat whole cell lysates. Jurkat cell lysates and quantities of purified Prxs were analysed by Western blotting in reducing conditions. Western blots are representative of 3 independent experiments. (**B**) Representative z-stack confocal images of a TMRE stained Jurkat cell (see Supplementary Movie S1 at http://www.BiochemJ.org/bj/421/bj4210051add.htm for an entire z-stack). The mitochondrial volume was calculated for each image in the z-stack. Five cells were quantified and the mitochondrial volume was calculated to be 15% (S.D. 3%).

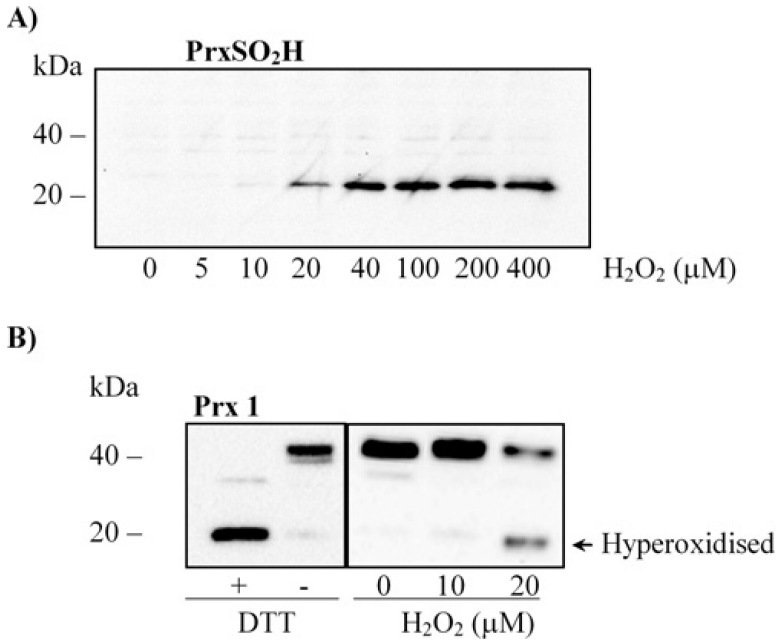

Figure 3. Redox immunoblot method to monitor Prx hyperoxidation

(**A**) Dose-dependent increase in Prx hyperoxidation in Jurkat cells exposed to hydrogen peroxide (0–400 μM). Prx hyperoxidation was monitored by Western blotting against Prx-SO_2H in non-reducing conditions. (**B**) Spontaneous dimerization of Prx 1 during cell harvest. Jurkat cells were harvested in extract buffer and analysed by Western blot in reducing (+DTT) or non-reducing (−DTT) conditions. Jurkat cells were exposed to hydrogen peroxide for 10 min before being harvested and examined by Western blot in non-reducing conditions. Western blots shown are representative of 3 independent experiments.

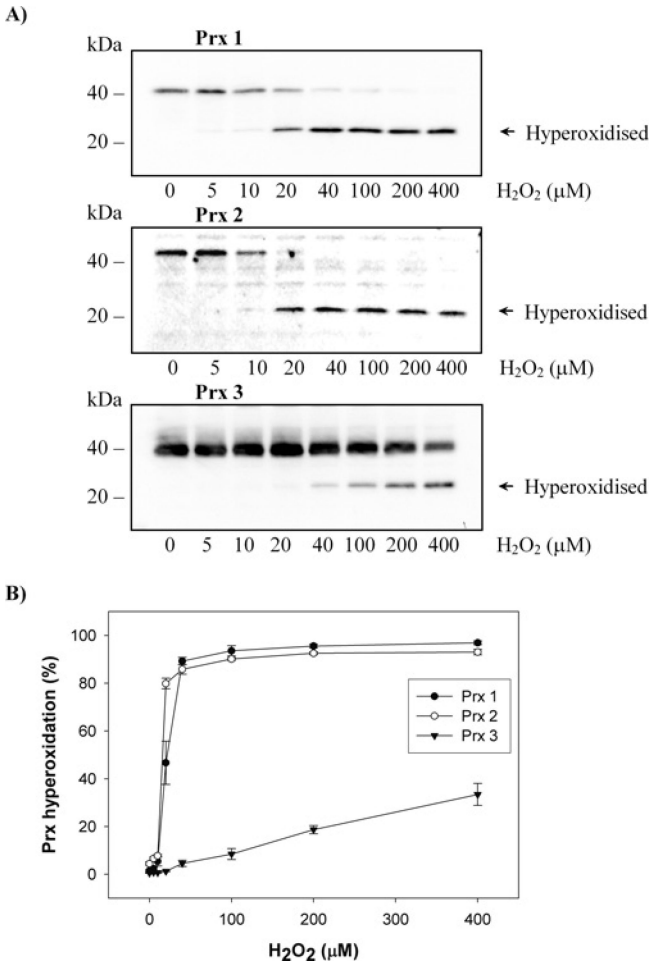

Figure 4. Differential susceptibility of Prxs to hyperoxidation in Jurkat cells exposed to hydrogen peroxide

(**A**) Jurkat cells were exposed to hydrogen peroxide (0–400 μM) for 10 min before being harvested in extract buffer and analysed by Western blot in non-reducing conditions. (**B**) The proportion of monomer (hyperoxidized) in each Western blot was analysed by Quantity One (Bio-Rad). Results represent the means ±S.E.M. of 3 independent experiments.

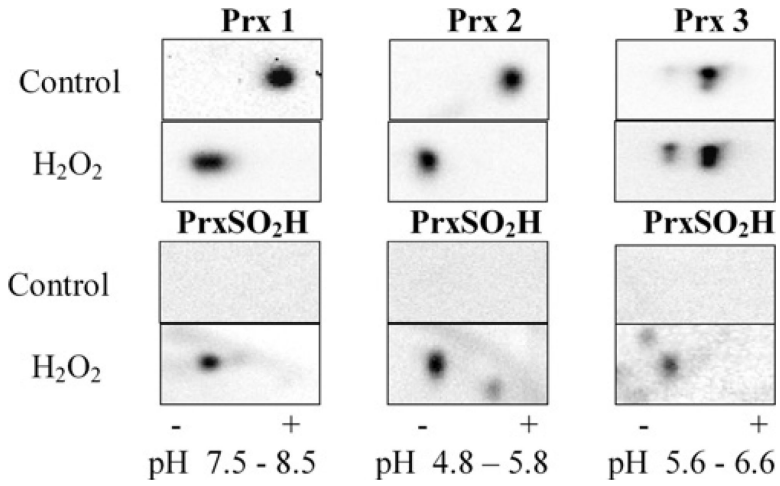

Figure 5. Verification of Prx hyperoxidation in Jurkat cells exposed to hydrogen peroxide

Jurkat cells were exposed to 200 μM hydrogen peroxide for 10 min before being harvested in extract buffer and resolved by 2D electrophoresis. Acidic shifts in Prx mobility were monitored by Western blot. Hyperoxidized Prx spots were validated by probing with the Prx-SO_2H antibody. The isoelectric regions for each isoform were as follows, Prx 1: pH 7.5−8.5, Prx 2: pH 4.8−5.8, Prx 3: pH 5.6−6.6. Western blots shown are representative of 3 independent experiments.

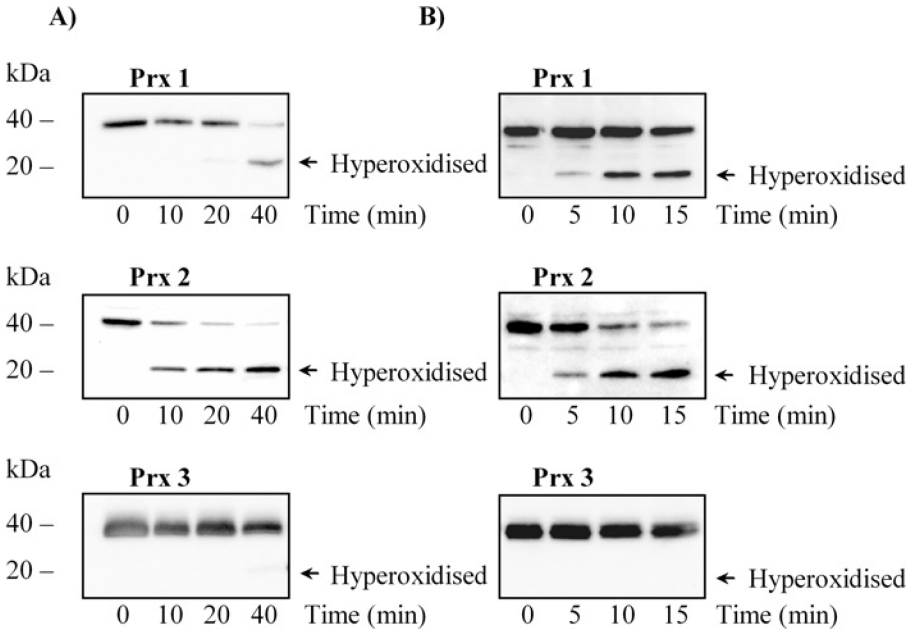

Figure 6. Differential susceptibility of Prxs to hyperoxidation in Jurkat cells exposed to either steady state hydrogen peroxide or UV-B radiation

(**A**) Time course of Prx hyperoxidation in Jurkat cells exposed to a steady-state level of hydrogen peroxide (10–15 μM). (**B**) Timecourse of Prx hyperoxidation in Jurkat cells exposed to UV-B radiation. Cells were exposed to steady-state hydrogen peroxide or UV-B radiation for various times before being harvested with extract buffer. Samples were analysed by Western blot in non-reducing conditions. Western blots shown are representative of 3 independent experiments.

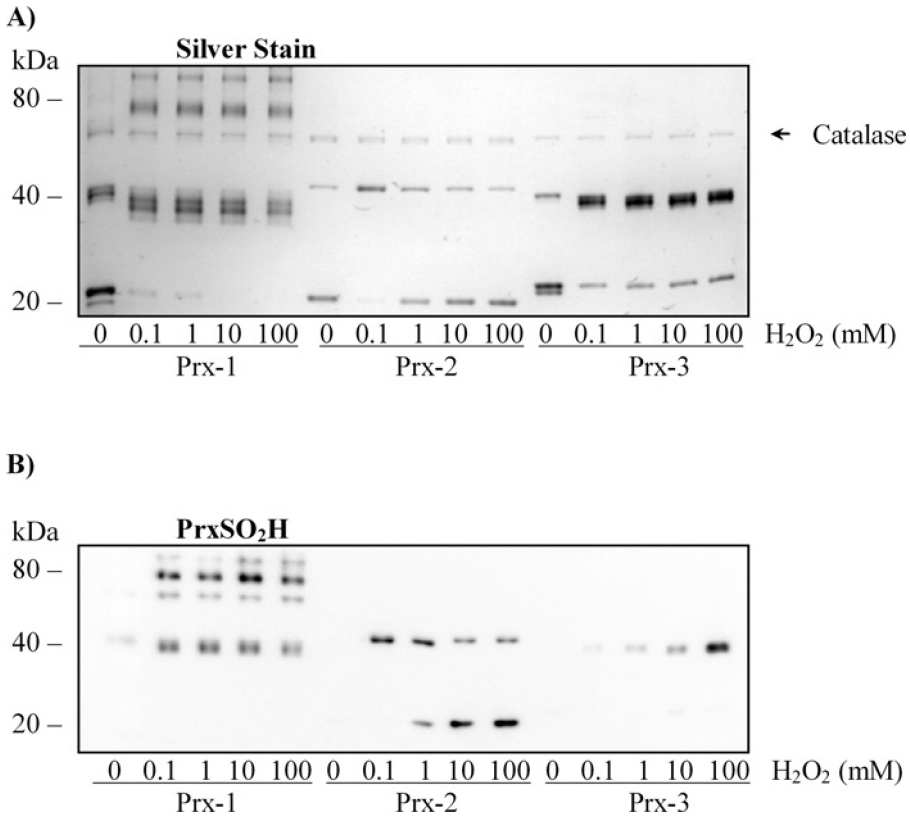

Figure 7. Differential susceptibility of purified Prxs to hyperoxidation

(**A**) Silver staining of reduced Prxs treated with hydrogen peroxide. (**B**) Immunodetection of Prx hyperoxidation. Reduced Prx 1, Prx 2 and Prx 3 (7 μM) were treated with hydrogen peroxide (0–100 mM) for 10 min, then 20 mM NEM and separated by SDS/PAGE under non-reducing conditions. A small amount of catalase, required to prevent re-oxidation of reduced Prxs, can be detected on the silver stain. All Prxs migrated as a monomer band under reducing conditions. A small amount of Prx-3 monomer failed to dimerize at any dose of H_2O_2. Protein gels and Western blots shown are representative of 3 independent experiments.

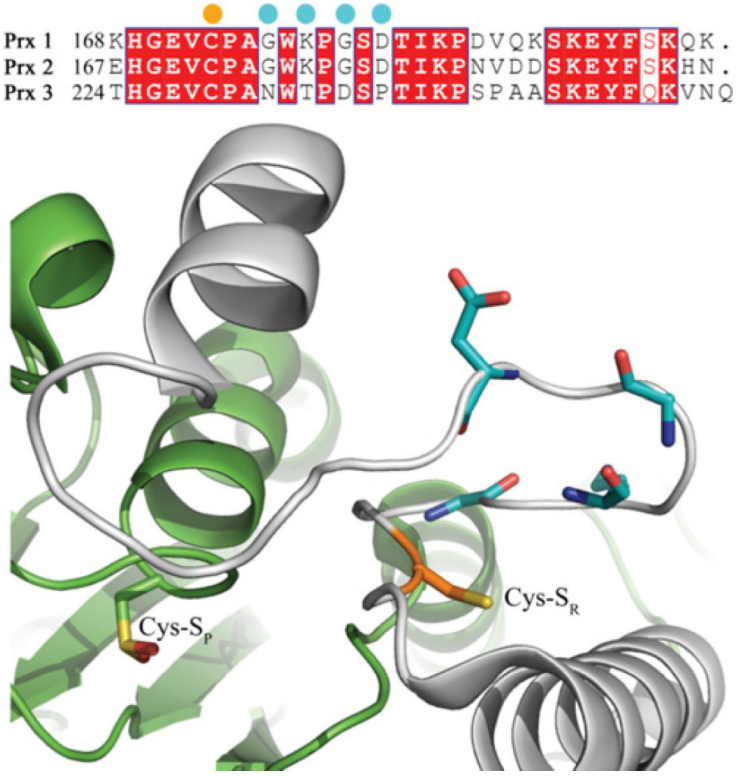

Figure 8. The unique C-terminal sequence of human Prx 3

The resolving Cys residue (Cys-S_R) and selected Prx 3 differences are highlighted in orange and cyan, respectively. The adjacent monomer of the Prx homodimer (green) contains the peroxidatic Cys residue (Cys-S_P). During normal catalysis, the C-terminus of the grey monomer rearranges to allow intermolecular disulfide bond formation. The structure shown is of human Prx 2 in the hyperoxidized state (PDB ID 1QMV) [48].